BMC Plant Biology

RESEARCH

Open Access

Temporal dynamics and optimal dose effects of biochar on soil properties, cotton growth, and bacterial community assembly in saline-alkali soils

Yuting Wang[1], Guangli Tian[2], Qingqing zhao[1], Dongwei Li[1,3*] and Shuai He[4*]

Abstract

Biochar is widely recognized as an effective soil amendment, yet its residual effects on saline soils remain underexplored. This study investigates the residual impact of a single biochar application on soil properties, bacterial community assembly, and cotton growth over three years. A controlled pot experiment was conducted using four biochar treatments – 0%, 1%, 3%, and 5% (w/w) - along with two cotton varieties: salt-sensitive and salt-tolerant. Results showed that biochar reduced soil salinity by 0.80–1.39 g·kg^{-1} in the second year, with no effects observed in years 1 and 3. By the third year, biochar at 5% increased soil pH by 0.34–0.44 units. Biochar application enhanced soil organic carbon by 135.15%–763.19%, total nitrogen by 12.88%–241.92%, and available potassium by 22.00%–168.84%, in a dose-dependent manner. However, available phosphorus was unaffected by biochar and showed a gradual decline over time. Biochar altered bacterial community composition but had limited impact on alpha diversity. A shift from homogeneous to heterogeneous selection in bacterial community assembly was observed in the third year, correlating with soil nutrient changes. Cotton growth exhibited an "A-shaped" response, with Limited benefits in the first and third years but improvement in the second year. The 1% biochar promoted cotton growth by at least 12.07%, whereas higher concentrations (3% and 5%) had no effect, emphasizing an optimal dose effect. These findings highlight biochar's potential as a tool for improving saline soils, while underscoring the importance of optimizing application rates and considering its long-term residual effects.

Keywords Biochar, Saline soil, Bacterial community, Cotton, Prolonged effects

*Correspondence:
Dongwei Li
lidongwei@caas.cn
Shuai He
xjshzhs@163.com
[1]Institute of Farmland Irrigation, Chinese Academy of Agricultural Sciences, 380 Hongli Avenue East, Xinxiang, Henan 453002, P.R. China
[2]Department of Agronomy and Horticulture, Jiangsu Vocational College of Agriculture and Forestry, Jurong 212400, China
[3]Institute of Western Agriculture, Chinese Academy of Agricultural Sciences, 831100 Changji, China
[4]Institute of Farmland Water Conservancy and Soil-fertilizer, Xinjiang Academy of Agricultural and Reclamation Science, Shihezi, Xinjiang 832000, P.R. China

Introduction

Soil salinization has emerged as a global agricultural crisis, currently affecting over 900 million hectares of arable land through structural degradation and nutrient availability impairment [1, 2]. In saline-alkali systems, high salinity impairs water uptake by plant roots and competitively inhibits the absorption of essential nutrients [3], while elevated osmotic pressure damages root membrane integrity [4, 5]. This ionic toxicity is further exacerbated by salt-induced microbial community collapse, characterized by reduced diversity and functional homogenization favoring halotolerant taxa [6]. Such environmental filtering critically disrupts microbially-mediated processes including organic matter mineralization and nitrogen cycling [7]. However, salinized soils hold significant potential for agricultural development and reutilization [8]. Developing ameliorated strategies to enhance microbial resilience and nutrient retention therefore represents an urgent sustainability priority.

Biochar derived from pyrolyzed agricultural residues (300–700 °C) functions as a multifunctional amendment for saline soils through synergistic mechanisms [9, 10]. The microporous structure effectively optimizes soil porosity architecture, significantly reduces bulk density, and enhances salt leaching efficiency while maintaining water retention capacity [11]. Surface charge dynamics regulate nitrogen and phosphorus availability via anion adsorption and pH-mediated solubilization [12], and labile carbon inputs combined with microhabitat complexity promote microbial community restructuring toward stress-resilient consortia [13, 14]. Critically, these beneficial properties evolve dynamically through microbially mediated aging processes [15], manifesting an intrinsic functional duality: while oxidation-generated surface oxygen groups enhance cation exchange capacity [16, 17], mineral deposition conversely occludes pores and reduces specific surface area [18]. This dual effect creates significant uncertainty regarding the persistence of biochar's benefits in saline systems subject to accelerated weathering. Current studies predominantly focus on immediate (< 1 year) amendment effects, leaving a critical knowledge gap in understanding the multi-year residual impacts on soil-microbe-plant interactions and biochar is irreversible once applied.

Cotton (*Gossypium hirsutum L.*) is a globally significant cash crop [19]. Its cultivation in arid and semi-arid regions faces severe salinity challenges, which constrain plant growth and yield [20]. As a pioneer species in salinized lands, cotton's growth serves as a valuable indicator of soil amelioration. Biochar enhances cotton growth by optimizing nutrient allocation [21], improving root architecture [9], and facilitating rhizosphere colonization by beneficial microbes [22]. However, studies demonstrate a well-defined dose threshold for these benefits, confined to optimal application rates [12, 23]. Excessive biochar application may lead to physical hindrance (e.g., hydrophobic biochar impeding root water absorption) [24], secondary salinization (e.g., mineral salts in biochar increasing soil electrical conductivity), and nutrient fixation (e.g., highly active surface functional groups in biochar binding to soil nutrients) [25], all of which can further limit crop growth. Biochar also influences soil microbial communities, which in turn affect nutrient cycling and overall plant health [26]. This microbial mediation introduces additional complexity to biochar's agronomic impacts. Therefore, it is crucial to apply biochar at the appropriate dosage, with careful consideration of its effects on microbial communities.

Based on the aforementioned knowledge gaps, addressing the uncertainties related to biochar aging and application rates is crucial for evaluating its effectiveness in soil remediation. This study conducted a three-year controlled experiment to fill this gap by investigating the multi-year impacts of biochar on the improvement of saline-alkali soils and cotton growth. The research integrates long-term data, dose analysis, and soil microbial ecology to provide a comprehensive understanding of biochar's effects on cotton growth. Specifically, the study aims to: (1) quantify the residual effects of single-dose biochar application (0%, 1%, 3%, 5% w/w) across multiple growing seasons, particularly in saline-alkali soils; (2) investigate how biochar aging influences microbial community dynamics and its subsequent impact on cotton growth. We hope that our research will provide critical insights into the longevity of biochar remediation effects, offering practical guidance for sustainable saline soil management strategies.

Materials and methods

Experiment site overview

The study was conducted from May to October each year, from 2021 to 2023, at the Experimental Station of Farmland Irrigation Research Institute (CAAS) under a rain-sheltered outdoor structure in Xinxiang, Henan Province (35°18′N, 113°54′E), China. This region exhibits a warm temperate continental monsoon climate characterized by distinct seasonal variations, with an annual mean temperature of 14 °C. The experimental site experiences a 210-day frost-free period and high annual evaporation reaching 2000 mm, creating typical semi-arid agricultural conditions.

Experimental materials

Soil samples were collected from the 0–20 cm layer of drip-irrigated cotton fields in Alar City, Xinjiang (40°22′–40°57′N, 80°30′–81°58′E). The sandy loam soil was air-dried, homogenized through 5-mm sieving, and stored under dry conditions prior to experimentation.

Corn straw-derived biochar produced via pyrolysis (500–600 °C) was obtained from Lize Environmental Technology Co., Ltd. (Henan). The essential physicochemical properties of the soil and biochar are detailed in Table 1. Two cotton cultivars (*Gossypium hirsutum L.*) with distinct salt tolerance were employed: the salt-sensitive (SS, *Medium S9612*) and the salt-tolerant (ST, *Medium 9807*), both sourced from the Institute of Cotton Research, CAAS (Anyang City, Henan Province, China).

Experimental design

A completely randomized 4 × 2 factorial design evaluated biochar application rates (0%, 1%, 3%, 5% w/w) and cotton varieties (SS vs. ST), generating eight treatments with 15 pots per treatment ($N = 120$). Cylindrical pots (Φ20 cm × 50 cm) were filled with 20 ± 0.5 kg soil column (40 ± 3 cm depth), with biochar homogenized in the 0–20 cm layer. Seeds were sown annually in May-June (2021–2023 schedules) and thinned to single uniform seedlings. Drip irrigation maintained 75%–90% of water holding capacity through weight-based water replenishment, Supplemented with 0.15 $g{\cdot}kg^{-1}$ N fertilizer (N: P_2O_5: K_2O = 5:3:4). Plant sampling commenced 35–40 days post-emergence for subsequent physiological analyses.

Sample collection

Soil samples

A 2 cm soil auger was used for sampling. Three pots (replicates) were randomly selected from the 15 pots per treatment. Each pot was sampled randomly using a 3-point sampling method at a soil depth of 0–20 cm. The samples were mixed, sieved (2-mm), and composite samples were prepared after removing roots and other impurities. The fresh soil samples were divided into three portions: one portion was immediately refrigerated at 4 °C for determining soil moisture content, nitrate and ammonium nitrogen; another portion was placed in centrifuge tubes, sealed with parafilm, and stored at −80 °C for DNA extraction and high-throughput sequencing; the final portion was air-dried for determining other basic chemical properties of the soil.

Plant samples

Morphometric parameters were systematically recorded: plant height (cm) using graduated rulers, and stem diameter (mm) at the first main stem node via digital caliper. Whole plants were then cleaned, Subjected to 105°C enzyme deactivation (30 min), followed by 75 °C drying to constant mass for aboveground biomass quantification. Since cotton growth was severely inhibited under the 5% biochar application rate treatment in the first year of the experiment (2021), no plant or soil samples were collected that year.

Soil chemical analysis

Soil pH was electrometrically determined at 1:5 (w/v) soil-water suspension using an FE28-Standard pH meter (Mettler Toledo). Total salt content (TSC) was quantified through steam drying methodology, while organic carbon (SOC) was analyzed via H_2SO_4-$K_2Cr_2O_7$ wet oxidation [27]. Total nitrogen (TN) was measured after H_2SO_4 digestion using an Auto Analyzer 3 system (Bran + Luebbe Inc., Norderstedt, Germany). Inorganic N species were extracted with 2 M KCl (1:4 soil: solution ratio, 200 rpm/1 h centrifugation) and quantified using an Auto Analyzer 3 system [28]. Available phosphorus (AP) followed Olsen's molybdate-blue protocol [29], using a UV-8000 spectrophotometer (Metash Instruments Co., Ltd., Shanghai, China). The available potassium (AK) content was extracted using 1 M NH_4OAc at pH 7 [30] and quantified using an FP640 flame photometer (Jqyiqi Co., Ltd., Shanghai, China).

DNA extraction and high-throughput sequencing

Total DNA was extracted from 0.5 g of fresh soil using the FastDNA® SPIN Kit for Soil (MP Biomedicals, USA) following the manufacturer's protocol. DNA integrity was checked via agarose gel electrophoresis, and purity/concentration were measured using a NanoDrop 2000 spectrophotometer (Thermo Fisher, USA) and Qubit 3.0 fluorometer (Invitrogen, USA). The V3-V4 region of the 16S rRNA gene was amplified using primers 341 F (5'-CCTACGGGNGGCWGCAG-3') and 805R (5'-GACTACHVGGGTATCTAATCC-3'). PCR products were validated by gel electrophoresis, purified with Agencourt AMPure XP beads, and sequenced using the Illumina NovaSeq 6000 platform (Illumina Inc., San Diego, CA, USA).

Processing and analysis of illumina sequencing data

Raw sequencing data were analyzed using QIIME 2 [31]. Adapter and primer sequences were removed using the

Table 1 The basic physical and chemical properties of biochar and soil

	pH	TSC ($g{\cdot}kg^{-1}$)	SOC ($g{\cdot}kg^{-1}$)	TN ($g{\cdot}kg^{-1}$)	TP ($g{\cdot}kg^{-1}$)	TK ($g{\cdot}kg^{-1}$)	Clay %	Silt %	Sand %
Soil	8.6	4.300	4.540	0.130	0.043	13.036	12.48	31.67	55.85
Biochar	9.0	/	410.898	8.354	2.327	30.594	/	/	/

The abbreviation in the table are as follows: *TSC* The salt content, *SOC* Soil organic carbon, *TN* Total nitrogen, *TP* Total phosphorus, *TK* Total potassium, *AP* Available phosphorus, *AK* Available potassium

cutadapt plugin, after which quality control and amplicon sequence variant (ASV) inference were carried out with DADA2 [32]. Taxonomic classification of the representative ASV sequences was achieved with a pre-trained Naïve Bayes classifier trained on the Ribosomal Database Project (version 11.5), with a confidence threshold set at 0.8 [33]. The raw sequencing data supporting the findings of this study have been deposited in the NCBI Sequence Read Archive (SRA) under the BioProject accession number PRJNA1321770.

Data analysis

The soil physicochemical parameters and growth metrics were depicted using line graphs, illustrating the differences in values between various biochar application rates and the control group (BC0) within the same planting year. In R, the ASV table was normalized using the "phyloseq" package. Then, the Chao1 and Shannon indices, representing the alpha diversity of the soil bacterial community, were calculated using the "microeco" package. Principal Coordinate Analysis (PCoA) was conducted using the "vegan" package to analyze the variation in bacterial community among different treatments. The correlation heatmap was created using the "heatmap" package in R.

The structuring of soil microbial communities was assessed using a null model implemented with the R packages "picante" and "ape" [34]. Specifically, we calculated the beta mean nearest-taxon distance (betaMNTD) between samples, and generated a null distribution by randomly shuffling the phylogenetic tree tip labels 999 times. The mean (mean_betaMNTD) and standard deviation (sd_betaMNTD) of this null distribution were then used to standardize the observed betaMNTD values for subsequent beta nearest taxon index (betaNTI) calculation, which reflects the phylogenetic dissimilarity among communities. In parallel, Bray–Curtis dissimilarity was used to calculate the modified Raup–Crick index (RC_{Bray}), representing the dissimilarity of community composition.

Based on these metrics, community ecological processes were classified according to the following criteria [35]: when |betaNTI| >2, deterministic processes were considered dominant, with betaNTI < −2 indicating homogeneous selection and betaNTI > 2 indicating heterogeneous selection. When |betaNTI| < 2 and $|RC_{Bray}|$ >0.95, probabilistic dispersal processes were considered dominant, where RC_{Bray} >0.95 indicated dispersal limited and RC_{Bray} < −0.95 indicated homogenizing dispersal. When |betaNTI| < 2 and $|RC_{Bray}|$ < 0.95, drift was considered the dominant process. The relative contributions of these five ecological processes were then quantified across all sample pairs.

Results

The residual effects of biochar on the soil chemical properties

Soil pH and salinity

In the first two years, soil pH remained stable across treatments (Fig. 1a; Fig. S1a, b). However, by the third year, the BC5 treatment increased soil pH by 0.34–0.44 units compared to the BC0 (Fig. 1a; Fig. S1c). Soil total salt content (TSC) was reduced by 0.80–1.39 $g{\cdot}kg^{-1}$ under biochar treatment specifically in year 2 relative to BC0, with no consistent reductions observed in years 1 and 3 (Fig. 1a; Fig. S1).

Soil nutrient contents

Biochar addition increased SOC, TN, and AK levels each year, showing a clear dosage effect - the greater the biochar application, the larger the increase (Fig. S2-S4). Compared to the BC0 control, SOC increased by 135.15%–763.19%, TN by 12.88%–241.92%, and AK by 22.00%–168.84%. The effects of biochar on SOC and TN remained stable over time (Fig. 1b). However, its impact on AK became more pronounced with longer duration (Fig. 1b). In contrast, biochar application exerted no impact on AP (Fig. S2b-S4b), yet AP depletion was more evident in biochar-treated groups over time (Fig. 1b). Biochar had no effect on inorganic nitrogen (nitrate and ammonia) in the first and third years (Fig. S2e-f; Fig. S4e-f). In the second year, biochar had no effect on nitrate nitrogen, but compared to the BC0 control, BC3 and BC5 reduced ammonia nitrogen by 64.78%–65.69% and 41.49%–50.32%, respectively (Fig. 1b; Fig. S3e-f).

The residual effects of biochar on the cotton growth

Biochar application exhibited an "A-shaped" effect on cotton growth parameters—including aboveground biomass, plant height, and stem diameter—with limited impact in the first and third years but enhancement in the second year (Fig. 1c). Integrating three-year data revealed an optimal dosage effect: at 1% biochar amendment, cotton growth Surpassed the control with biomass, height, and stem thickness increasing by 24.13%–80.72%, 12.07%–29.65%, and 13.99%–33.22% respectively (Fig. 1c; Fig. S5). However, higher application rates (3%–5%) exerted no detectable effects on cotton growth (Fig. 1c; Fig. S5). Notably, cotton growth indicators declined over time with continuous planting (Fig. S6a).

Residual effects of Biochar on soil bacterial communities

Soil bacterial community characteristics

Changes in Chao1 and Shannon indices showed that biochar had no impact on bacterial alpha diversity within the same cropping year (Fig. 2a, S7). The only exception was a reduction in diversity under BC5 in the second year the ST variety, where Chao1 and Shannon indices

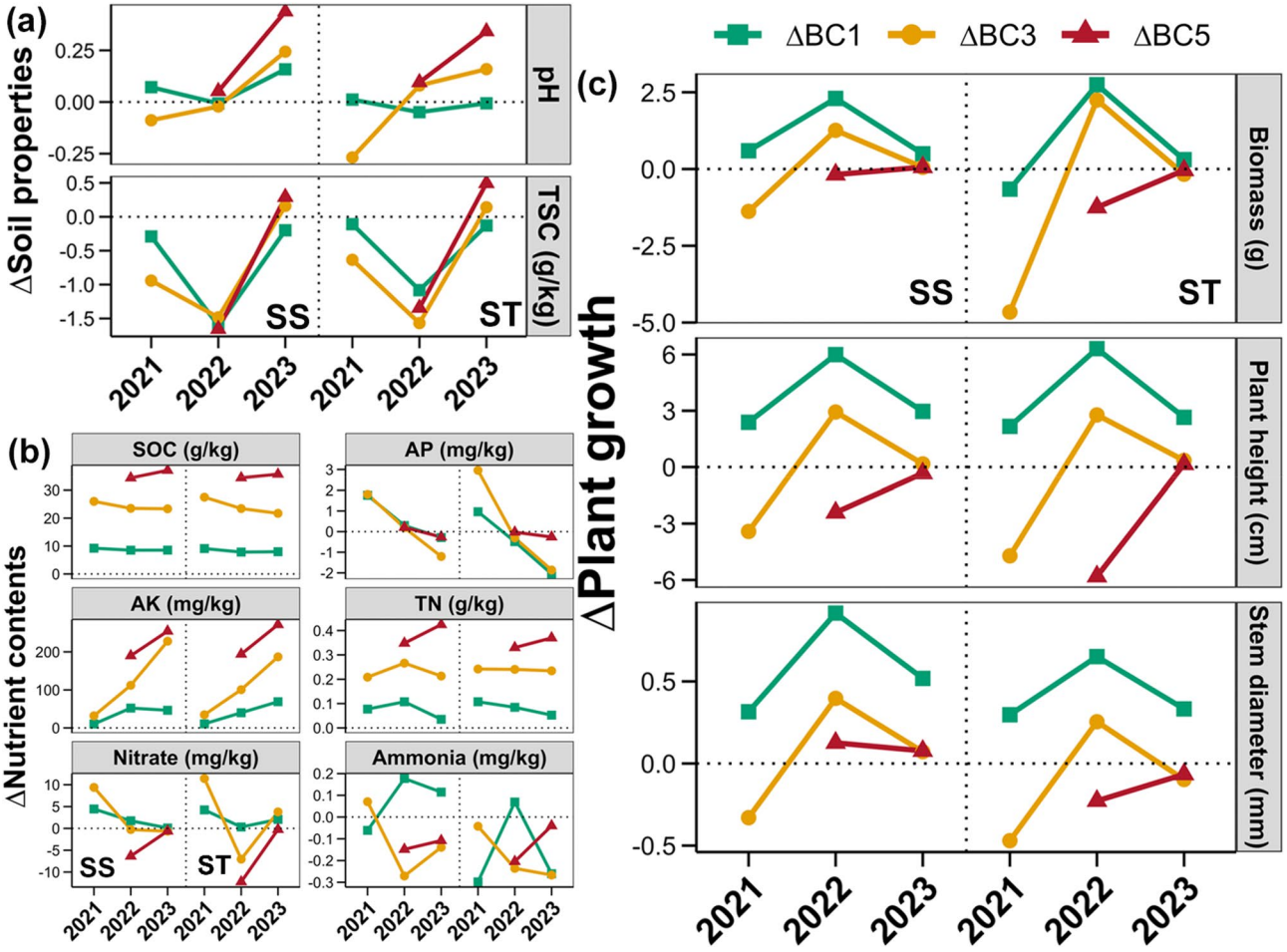

Fig. 1 In the years 2021–2023, the differences between different biomass charcoal addition groups and their respective control groups for the same planting year were observed in soil pH and salinity (**a**), soil nutrients (**b**), and cotton growth (**c**). In the figure, TSC stands for total soil salinity, SOC represents soil organic carbon, AP denotes available phosphorus, AK indicates available potassium, and TN refers to total nitrogen

decreased by 7.91%–35.09% and 1.53%–6.44%, respectively (Fig. S7). Correlation analysis further showed that soil pH, salinity, and available phosphorus negatively correlated with bacterial diversity, while available potassium and nitrate nitrogen had positive associations (Fig. 2b).

Principal coordinate analysis (PCoA) based on Bray-Curtis distances showed that bacterial community composition clustered primarily by planting year (Fig. 2c). An adonis test confirmed that cropping duration exerted the strongest effect ($R^2 = 0.202$, $p < 0.001$), followed by biochar amendment ($R^2 = 0.067$, $p < 0.001$), whereas cotton variety had no influence (Fig. 2c). Within individual years, biochar-treated samples tended to cluster together along the PC1 axis (Fig. 2c).

Soil bacterial community assembly

Null model analysis showed that biochar addition influenced soil bacterial community assembly over time (Fig. 3a). Deterministic processes remained dominant, but betaNTI values indicated a shift in selection mechanisms. In the first two years, betaNTI values were below −2, with homogeneous selection accounting for 62.09% and 67.03%, respectively (Fig. 3a, b). By the third year, values exceeded 2, happening a transition to heterogeneous selection, which accounted for 84.06% (Fig. 3a, b). Further correlation analysis showed that the association between betaNTI and nutrient contents ($R^2 = 0.353$, $p < 0.001$) was stronger than that with soil properties (including pH and salinity, $R^2 = 0.026$, $p < 0.001$; Fig. 3c, d).

Relationship between soil environment and cotton growth

Contribution of soil bacterial diversity and community composition

Spearman correlation analysis showed a relationship between soil bacterial alpha diversity and cotton growth (Fig. 4a). When data from all three years were combined, bacterial alpha diversity showed a negative correlation with cotton growth indicators, though no correlation was detected in any individual year (Fig. 4a). A random

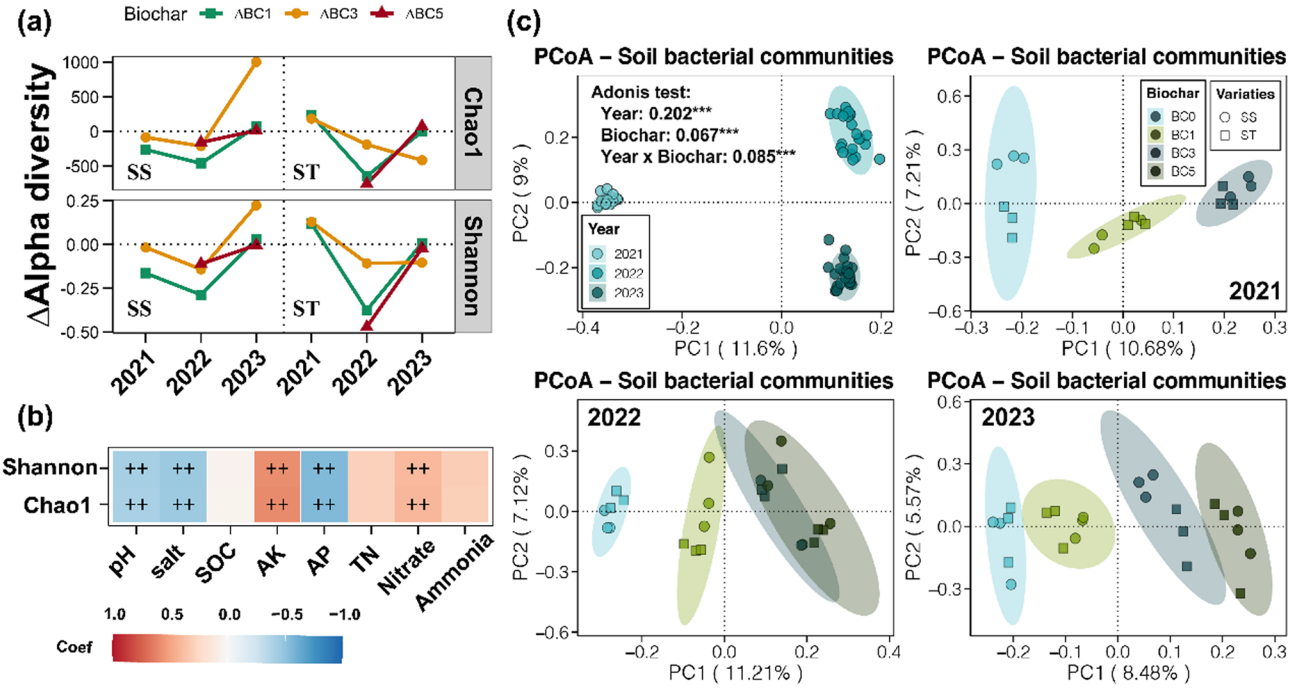

Fig. 2 In the years 2021–2023, the differences between different biomass charcoal addition groups and their respective control groups for the same planting year were observed in soil bacterial alpha diversity (**a**), the correlation between soil chemical properties and soil bacterial alpha diversity (**b**), and the differences in soil bacterial communities among different biochar types, cotton varieties, and planting years (**c**)

forest model based on phylum-level bacterial composition Successfully distinguished soil samples from different cropping years with 100% accuracy (Fig. 4b). Further modeling demonstrated that bacterial composition could predict cotton growth indicators, with over 70% accuracy for above-ground biomass and plant height, and approximately 60% for stem thickness (Fig. 4c, Fig. S8a, c). Notably, the bacterial phyla Verrucomicrobiota, Entotheonellaeota, and Bacteroidota appeared in all three models, with their relative abundances varying across different planting durations (Fig. 4d, Fig. S8b, d).

Linkage between soil bacterial community assembly and cotton growth

Analysis of the association between soil bacterial phylogenetic distances and cotton growth showed that all treatments, except for BC1, exhibited correlations (Fig. 5a). The null model indicated that deterministic processes primarily shaped the bacterial community across different biochar treatments, with heterogeneous selection accounting for 59.09%–75.16% (Fig. 5b). Homogeneous selection contributed 18.3%–25.76%, while stochastic processes accounted for 3.92%–17.65%. Notably, ecological drift was a significant factor in the BC1 group, contributing around 10%, whereas it was nearly absent in the other treatments (Fig. 5b).

Discussion

The dynamic regulation of biochar on soil chemical properties

The residual effects of biochar on regulating soil chemical properties exhibited significant temporal heterogeneity (Fig. 1a, b). In the second year after biochar application, soil salinity decreased (Fig. 1a; Fig. S1), which was associated with the porous structure of biochar promoting salt leaching [36]. However, the salinity mitigation effect diminished in the third year (Fig. S1), potentially due to biochar aging, which may result in the release of colloidal/nano-sized biochar particles [37] or degradation of surface pore structures [38], leading to soil pore clogging. The phased increase in soil pH (Fig. S1c) likely resulted from the gradual release of alkaline components such as carbonate-bound calcium and magnesium from biochar [39], while the short-term buffering effect disappeared.

Nutrient deficiency constitutes another major limiting factor in saline-alkali soils. Biochar, characterized by high nutrient content and a porous structure, can effectively enhance soil fertility [40]. In this study, the employed biochar exhibited substantially higher SOC (410.898 $g{\cdot}kg^{-1}$) and TN (8.354 $g{\cdot}kg^{-1}$) contents compared to the initial soil baseline (Table 1). Consequently, biochar application significantly increased SOC and TN concentrations in a dose-dependent manner (Fig. 1b; Fig. S2-S4), which aligns with the findings reported by Dai et al. [41]. The subsequent decline in structural integrity gradually

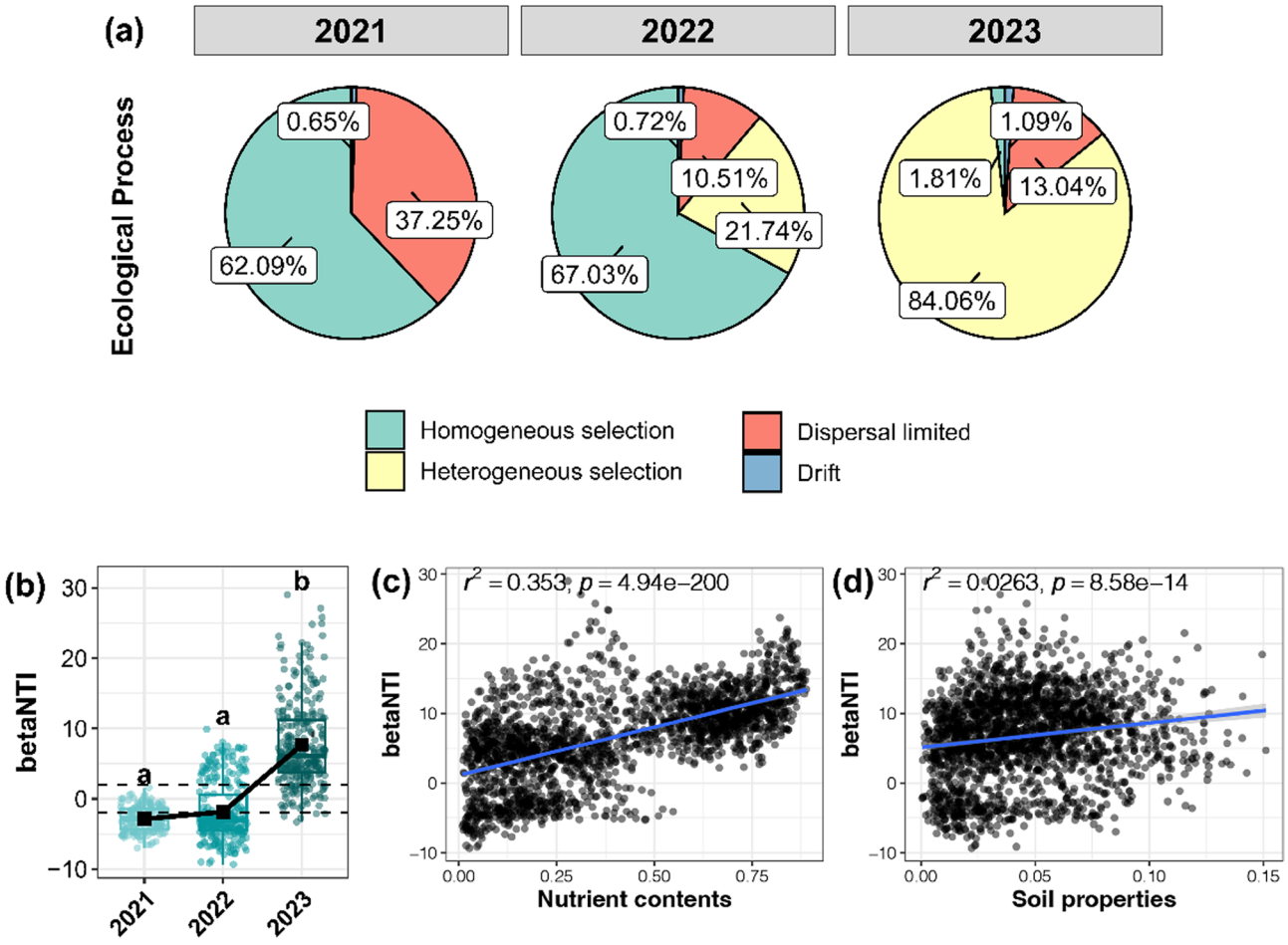

Fig. 3 In the years 2021–2023, the ecological processes underlying the assembly of soil bacterial communities (**a**), changes in beta-nearest taxon index (betaNTI) based on null models (**b**), and the relationship between soil properties and betaNTI (**c**)

compromised biochar' phosphorus retention capacity over time [42]. Furthermore, biochar residues altered the soil redox status, which led to elevated soil pH and promoted the transformation of phosphorus into less bioavailable forms [43]. Our data are consistent with this finding, as the observed increase in pH during the third year likely contributed to the decline in available phosphorus levels (Fig. 1b). Long-term monoculture may lead to nutrient depletion and pathogen accumulation [44, 45]. In particular, the content of available phosphorus decreases year by year (Fig. 1b), which is also the reason for the annual decline in plant biomass (Fig. S6a).

Residual effects of biochar on the soil bacterial community

Biochar enhances the growth of specific carbon-degrading bacteria by serving as a carbon substrate, while its alkaline properties potentially reduce the abundance of acidophilic bacterial taxa [46, 47]. The increased abundance of dominant bacterial populations may suppress the growth of other bacterial groups, consequently leading to reduced bacterial diversity. However, discrepancies exist among different studies [48, 49], as environmental factors selectively promote the growth of certain microorganisms, thereby influencing bacterial community diversity. In this study, bacterial alpha diversity showed negative correlations with pH, salinity, and available phosphorus, but positive correlations with available potassium and nitrate nitrogen (Fig. 2b), demonstrating the crucial role of soil environmental conditions in shaping microbial diversity.

Residual effects of biochar on the soil bacterial community assembly

The assembly of soil microbial communities is mediated by both deterministic and stochastic processes, with their relative importance being context-dependent [50]. Results from null model analyses revealed that deterministic processes predominated in shaping microbial community assembly throughout the three-year experiment (Fig. 3a). These deterministic mechanisms primarily reflect microbial adaptive responses to environmental conditions, manifested through both habitat

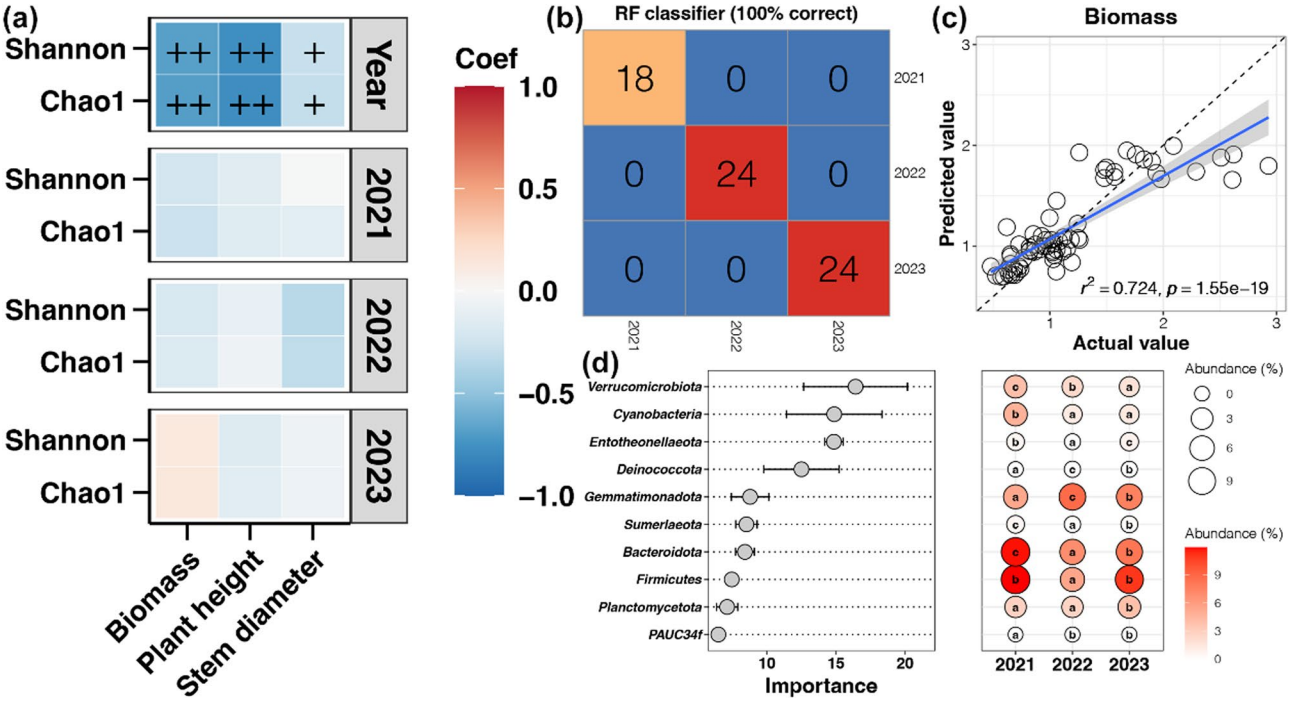

Fig. 4 The correlation between soil bacterial alpha diversity and cotton growth indicators (**a**), the use of a random forest model to distinguish samples from the continuous planting process based on soil bacterial composition (**b**), the prediction of aboveground biomass of cotton using a random forest model based on phylum-level species composition (**c**), and the important species and relative abundance changes affecting cotton biomass (**d**)

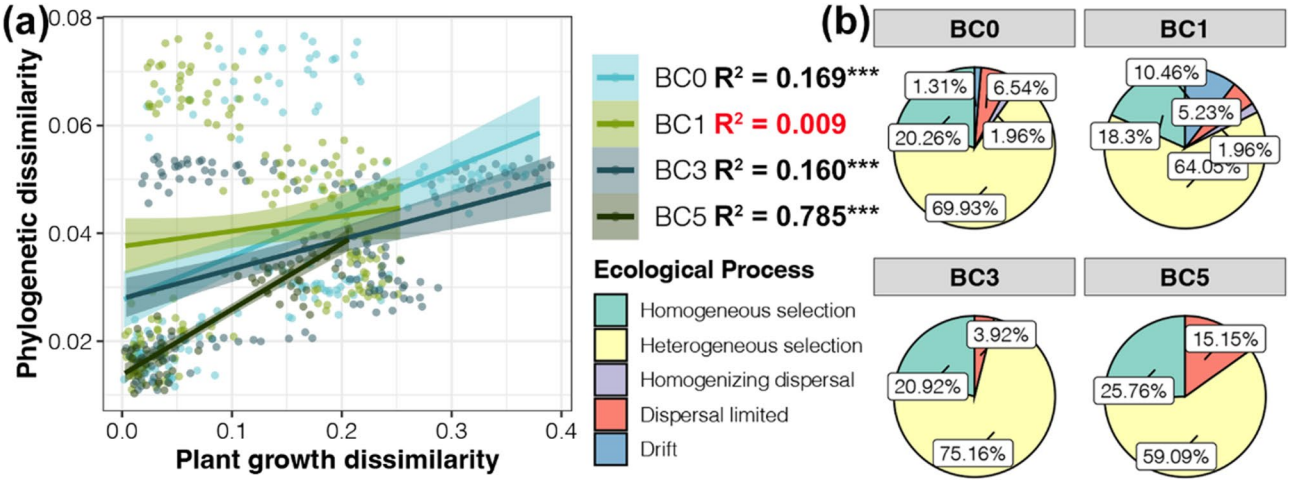

Fig. 5 The association between the phylogenetic development of soil bacterial communities and changes in cotton growth status (**a**), and the ecological processes underlying the assembly of soil bacterial communities under different biomass charcoal addition levels, based on null models (**b**)

specialization (including species-specific niche preferences) and environmental filtering [51]. Our study demonstrates that soil nutrients exert significantly stronger influences than pH and salinity on bacterial community assembly (Fig. 3c), highlighting their pivotal role as key drivers in structuring soil microbial communities. However, other studies have reported that soil salinity exerts a strong selective pressure on bacterial community assembly in coastal estuarine wetlands [52]. These divergent findings underscore the geographic and environmental specificity of microbial assembly processes across different soil ecosystems.

Focusing on the legacy effects of biochar on ecological selection processes, our results demonstrate that community assembly during the initial two years was strongly driven by homogeneous selection (Fig. 3a, b). This deterministic process preferentially enriched microbial populations with conserved functional profiles and convergent adaptive traits, reflecting environmental filtering under biochar amendment [51]. However, by the third year,

heterogeneous selection became the dominant process (Fig. 3a, b), potentially reflecting adaptive changes in the soil environment under long-term monocropping pressure. This shift may be related to increased phosphorus limitation during the third year of cultivation (Fig. 1b). The result reveals the dynamic adaptability of microbial communities to long-term environmental changes while also highlighting the importance of the temporal scale in understanding community assembly processes.

Effects of biochar application rate and time on cotton growth

Biochar exhibits a non-monotonic dose response coupled with temporal dynamics in regulating cotton growth (Fig. S5-S6). Low-dose application (1% w/w) significantly enhances biomass accumulation, plant height, and stem diameter (Fig. S5). However, higher application rates (3% and 5%) may impede root development through physical pore obstruction [53], consistent with reported nitrogen uptake inhibition under excessive application (> 80 t ha^{-1}) [54]. Furthermore, biochar exhibited an "A-shaped" interannual fluctuation pattern in its effects on cotton growth (Fig. 1c). In the first year, a slow-release priming effect predominated [55], followed by the strongest growth promotion in the second year due to improved salinity regulation. By the third year, however, the benefits were substantially diminished by phosphorus limitation and long-term monoculture.

Under biochar amendment, cotton growth was closely associated with shifts in bacterial community composition, while alpha diversity showed no clear link (Fig. 4a, b, and c), suggesting that community restructuring may be more influential in saline–alkali soils. Random forest modeling revealed that phylum-level composition could predict 60%–70% of growth performance metrics (Fig. 4c; Fig. S8). Under the 1% biochar amendment, the association between soil bacterial phylogenetic composition and cotton growth was not evident (Fig. 5a), suggesting that the improvement in cotton growth was driven by the optimization of soil physicochemical properties (e.g., reduced salinity and enhanced nutrient availability) or by the response of specific functional taxa, rather than by shifts in phylogenetic structure. Concurrently, the relative contribution of ecological drift increased to 10% (Fig. 5b). An elevated proportion of drift typically arises under conditions of reduced environmental selection pressure [56], thereby providing cotton with greater opportunities to recruit beneficial microorganisms during growth.

Despite the promising preliminary findings, this study has several limitations. The effects of biochar followed a distinct temporal trajectory, highlighting the need for extended field experiments and long-term monitoring (5–10 years) to fully assess its agronomic benefits and environmental consequences. Moreover, elucidating the mechanisms by which biochar interacts with soil microbial communities—and how these interactions underpin cotton growth—remains a critical avenue for future research.

Conclusion

This study demonstrates that biochar's ameliorative effects on saline-alkali soils exhibit an optimal dose effect and temporal dynamics, with a 1% (w/w) application rate promoting cotton growth, while higher doses had no effect. In the second year, the 1% biochar treatment also reduced soil salinity, leading to the most significant growth promotion. Although biochar continuously increased SOC, TN, and AK levels, its salinity alleviation effect disappeared by the third year, and AP decreased over time, which was associated with an increase in soil pH and contributed to the decline in cotton growth, highlighting the temporal dynamics of biochar's impact. Microbial community assembly shifted decisively from homogeneous selection to heterogeneous dominance in the third year, paralleling the emergence of growth decline. These results highlight biochar's potential to improve soil fertility and cotton growth, while emphasizing that integrating temporal effects with biochar amendments may help maintain microbial balance and prevent crop growth limitations.

Supplementary Information

The online version contains supplementary material available at https://doi.org/10.1186/s12870-025-07415-8.

Supplementary Material 1. Fig. S1 Variation patterns of soil pH and TSC under different treatments in 2021 (a), 2022 (b), and 2023 (c). Different lowercase letters indicate significant differences among treatments ($p < 0.05$). TSC stands for total soil salinity. Fig. S2 Variation patterns of soil nutrients under different treatments in 2021: SOC (a), AP (b), AK (c), TN (d), Nitrate (e), and Ammonia (f). Different lowercase letters indicate significant differences among treatments ($p < 0.05$). SOC represents soil organic carbon, AP denotes available phosphorus, AK indicates available potassium, and TN refers to total nitrogen. Fig. S3 Variation patterns of soil nutrients under different treatments in 2022: SOC (a), AP (b), AK (c), TN (d), Nitrate (e), and Ammonia (f). Different lowercase letters indicate significant differences among treatments ($p < 0.05$). SOC represents soil organic carbon, AP denotes available phosphorus, AK indicates available potassium, and TN refers to total nitrogen. Fig. S4 Variation patterns of soil nutrients under different treatments in 2023: SOC (a), AP (b), AK (c), TN (d), Nitrate (e), and Ammonia (f). Different lowercase letters indicate significant differences among treatments ($p < 0.05$). SOC represents soil organic carbon, AP denotes available phosphorus, AK indicates available potassium, and TN refers to total nitrogen. Fig. S5 Variations in biomass, plant height, and stem diameter under different biochar treatments in 2021 (a), 2022 (b), and 2023 (c). Different lowercase letters indicate significant differences among treatments ($p < 0.05$). Fig. S6 Temporal variations in biomass, plant height, and stem diameter during 2021-2023 (a). Variation patterns of biomass, plant height and stem diameter among different biochar treatments (b). Different lowercase letters indicate significant differences among treatments ($p < 0.05$). Fig. S7 Effects of biochar on bacterial alpha diversity within the same growing season. Different lowercase letters indicate significant differences among treatments ($p< 0.05$). Fig. S8 Predictive analysis of bacterial community composition on cotton plant height (a) and stem diameter (c). Random forest function prediction (b, d). Different lowercase letters indicate significant differences among treatments ($p < 0.05$).

Acknowledgements
Not applicable.

Authors' contributions
Y.W. wrote the main manuscript text. G.T. contributed to the work design and data analysis. Q.Z. contributed to data gathering and data administration. D.L. drafted the work or substantively revised it. S.H. contributed to the study design and manuscript editing. All authors reviewed the manuscript.

Funding
This work was financed by the Agricultural Science and Technology Innovation Program (ASTIP) of Chinese Academy of Agricultural Sciences, and the Key Technological Research and Development Initiative for Priority Areas in Divisions and Cities of XPCC (No. KY2024GG09).

Data availability
The datasets used and/or analysed during the current study are available from the corresponding author on reasonable request.

Declarations

Ethics approval and consent to participate
Not applicable.

Consent for publication
Not applicable.

Competing interests
The authors declare no competing interests.

Received: 10 June 2025 / Accepted: 12 September 2025
Published online: 08 October 2025

References

1. Cui Q, Xia J, Yang H, Liu J, Shao P. Biochar and effective microorganisms promote *Sesbania cannabina* growth and soil quality in the coastal saline-alkali soil of the Yellow River Delta, China. Sci Total Environ. 2021;756:143801. https://doi.org/10.1016/j.scitotenv.2020.143801.
2. Xin Y, Wu Y, Zhang H, Li X, Qu X. Soil depth exerts a stronger impact on microbial communities and the sulfur biological cycle than salinity in salinized soils. Sci Total Environ. 2023;894:164898. https://doi.org/10.1016/j.scitotenv.2023.164898.
3. Cavalcante JSJ, Ferreira Neto M, Peixoto TDC, Pereira KTO, Umbelino BF, Rodrigues Filho RA, et al. Production, growth, photosynthetic response, and ionic responses of arugula cultivars under salt stress elicitors. J Plant Growth Regul. 2025. https://doi.org/10.1007/s00344-025-11823-3.
4. Chen Q, Cao X, Li Y, Sun Q, Dai L, Li J, et al. Functional carbon nanodots improve soil quality and tomato tolerance in saline-alkali soils. Sci Total Environ. 2022;830:154817. https://doi.org/10.1016/j.scitotenv.2022.154817.
5. Yin Z, Wang X, Hu Y, Zhang J, Li H, Cui Y, et al. Metabacillus dongyingensis sp. Nov. Is represented by the plant growth-Promoting bacterium BY2G20 isolated from Saline-Alkaline soil and enhances the growth of Zea Mays L. Under Salt Stress mSystems. 2022;7:e0142621. https://doi.org/10.1128/msystems.01426-21.
6. Wang X, Riaz M, Babar S, Eldesouki Z, Liu B, Xia H, et al. Alterations in the composition and metabolite profiles of the saline-alkali soil microbial community through biochar application. J Environ Manage. 2024;352:120033. https://doi.org/10.1016/j.jenvman.2024.120033.
7. Kong W, Wei X, Wu Y, Shao M, Zhang Q, Sadowsky MJ, et al. Afforestation can lower microbial diversity and functionality in deep soil layers in a semiarid region. Glob Change Biol. 2022;28:6086–101. https://doi.org/10.1111/gcb.16334.
8. Zou H, Shi Z, Liu J, Wang J, Li P. Saline-alkali resilience: the role of *Trametes* NF1 in promoting alfalfa growth and salinity tolerance. Int Microbiol. 2025. https://doi.org/10.1007/s10123-025-00680-5.
9. Hou J, Wan H, Liang K, Cui B, Ma Y, Chen Y, et al. Biochar amendment combined with partial root-zone drying irrigation alleviates salinity stress and improves root morphology and water use efficiency in cotton plant. Sci Total Environ. 2023;904:166978. https://doi.org/10.1016/j.scitotenv.2023.166978.
10. Liu Z, Zhang W, Ma R, Li S, Song K, Zheng J, et al. Biochar-plant interactions enhance nonbiochar carbon sequestration in a rice paddy soil. Commun Earth Environ. 2023;4:494. https://doi.org/10.1038/s43247-023-01155-z.
11. Su Z, Liu X, Wang Z, Wang J. Biochar effects on salt-affected soil properties and plant productivity: a global meta-analysis. J Environ Manage. 2024;366:121653. https://doi.org/10.1016/j.jenvman.2024.121653.
12. Wang Y, Tian G, Qiu H, Zhou X, Zhao Q, Tian Y, et al. Biochar drives changes in soil bacterial communities and cotton growth by improving nutrients availability under saline conditions. Land Degrad Dev. 2024;35:1335–51. https://doi.org/10.1002/ldr.4990.
13. Kerner P, Struhs E, Mirkouei A, Aho K, Lohse KA, Dungan RS, et al. Microbial responses to biochar soil amendment and influential factors: a three-level meta-analysis. Environ Sci Technol. 2023;57:19838–48. https://doi.org/10.1021/acs.est.3c04201.
14. Li M, Long T, Tian K, Wei C, Liu M, Wu M, et al. Temperature and moisture mediated changes in chemical and microbial properties of biochars in an anthrosol. Sci Total Environ. 2022;845:157219. https://doi.org/10.1016/j.scitotenv.2022.157219.
15. Chen X, Jiang S, Wu J, Yi X, Dai G, Shu Y. Three-year field experiments revealed the immobilization effect of natural aging biochar on typical heavy metals (Pb, cu, Cd). Sci Total Environ. 2024;912:169384. https://doi.org/10.1016/j.scitotenv.2023.169384.
16. Feng Y, Feng Y, Liu Q, Chen S, Hou P, Poinern G, et al. How does biochar aging affect NH3 volatilization and GHGs emissions from agricultural soils? Environ Pollut. 2022;294:118598. https://doi.org/10.1016/j.envpol.2021.118598.
17. Wang L, Gao C, Yang K, Sheng Y, Xu J, Zhao Y, et al. Effects of biochar aging in the soil on its mechanical property and performance for soil CO2 and N2O emissions. Sci Total Environ. 2021;782:146824. https://doi.org/10.1016/j.scitotenv.2021.146824.
18. Wang L, O'Connor D, Rinklebe J, Ok YS, Tsang DCW, Shen Z, et al. Biochar aging: mechanisms, physicochemical changes, assessment, and implications for field applications. Environ Sci Technol. 2020;54:14797–814. https://doi.org/10.1021/acs.est.0c04033.
19. Zhang Z, Huang J, Yao Y, Peters G, Macdonald B, La Rosa AD, et al. Environmental impacts of cotton and opportunities for improvement. Nat Rev Earth Environ. 2023;4:703–15. https://doi.org/10.1038/s43017-023-00476-z.
20. Wang X, Riaz M, Xia X, Babar S, El-Desouki Z, Li Y, et al. Alleviation of cotton growth suppression caused by salinity through biochar is strongly linked to the microbial metabolic potential in saline-alkali soil. Sci Total Environ. 2024;922:171407. https://doi.org/10.1016/j.scitotenv.2024.171407.
21. Jin W, Liu Z, Wang Q, Cheng Z, Zhang Y, Cao N, et al. Straw-derived biochar incorporation improves seedcotton yield and fiber quality by optimizing photosynthetic carbon and nutrients partitioning and boll formation patterns. Ind Crops Prod. 2024;214:118617. https://doi.org/10.1016/j.indcrop.2024.118617.
22. Wang J, Riaz M, Babar S, El-Desouki Z, Li Y, Wang X, et al. Iron-modified biochar enhances cotton growth and iron uptake in saline-alkali soil by reducing salinity and facilitating root colonization of beneficial bacteria. Plant Soil. 2025. https://doi.org/10.1007/s11104-025-07415-5.
23. Wang X, Li Y, Wang H, Wang Y, Biswas A, Wai Chau H, et al. Targeted biochar application alters physical, chemical, hydrological and thermal properties of salt-affected soils under cotton-sugarbeet intercropping. CATENA. 2022;216:106414. https://doi.org/10.1016/j.catena.2022.106414.
24. Cox J, Jenkins A, Hickey M, Lines-Kelly R, McClintock A, Powell J et al. Biochar in horticulture: prospects for the use of Biochar in Australian horticulture. Investment. 2015.Cox J, Jenkins A, Hickey M, Lines-Kelly R, McClintock A, Powell J et al. Biochar in Horticulture: Prospects for the use of Biochar in Australian horticulture; NSW Department of Primary Industries: Sydney, Australia, 2012; pp. 1–104.
25. Antonangelo JA, Sun X, de Eufrade-Junior H. Biochar impact on soil health and tree-based crops: a review. Biochar. 2025;7:51. https://doi.org/10.1007/s42773-025-00450-6.
26. Hu W, Zhang Y, Rong X, Zhou X, Fei J, Peng J, et al. Biochar and organic fertilizer applications enhance soil functional microbial abundance and agroecosystem multifunctionality. Biochar. 2024;6:3. https://doi.org/10.1007/s42773-023-00296-w.
27. Nelson DW, Sommers LE, Total, Carbon. Organic carbon, and organic matter. Methods of soil analysis. John Wiley & Sons, Ltd; 1996. pp. 961–1010. https://doi.org/10.2136/sssabookser5.3.c34.
28. Keeney Dr. Nelson D w. Nitrogen—Inorganic forms. Methods of soil analysis. John Wiley & Sons, Ltd; 1982. pp. 643–98. https://doi.org/10.2134/agronmonogr9.2.2ed.c33.

29. Silva CSD, Koralage ISA, Weerasinghe P, Silva NRN. The determination of available phosphorus in soil: a quick and simple method. OUSL Journal. 2015;8:undefined-undefined. https://doi.org/10.4038/ouslj.v8i0.7315.
30. Zebec V, Rastija D, Lončarić Z, Bensa A, Popović B, Ivezić V. Comparison of chemical extraction methods for determination of soil potassium in different soil types. Eurasian Soil Sci. 2017;50:1420–7. https://doi.org/10.1134/S1064229317130051.
31. Bolyen E, Rideout JR, Dillon MR, Bokulich NA, Abnet CC, Al-Ghalith GA, et al. Reproducible, interactive, scalable and extensible microbiome data science using QIIME 2. Nat Biotechnol. 2019;37:852–7. https://doi.org/10.1038/s41587-019-0209-9.
32. Callahan BJ, McMurdie PJ, Rosen MJ, Han AW, Johnson AJA, Holmes SP. DADA2: High-resolution sample inference from illumina amplicon data. Nat Methods. 2016;13:581–3. https://doi.org/10.1038/nmeth.3869.
33. Zhu J, Niu W, Zhang Z, Siddique KHM, Dan Sun, Yang R. Distinct roles for soil bacterial and fungal communities associated with the availability of carbon and phosphorus under aerated drip irrigation. Agric Water Manage. 2022;274:107925. https://doi.org/10.1016/j.agwat.2022.107925.
34. Zhang Z, Deng Y, Feng K, Cai W, Li S, Yin H, et al. Deterministic assembly and diversity gradient altered the biofilm community performances of bioreactors. Environ Sci Technol. 2019;53:1315–24. https://doi.org/10.1021/acs.est.8b06044.
35. Zhou J, Ning D. Stochastic community assembly: does it matter in microbial ecology? Microbiol Mol Biol Rev. 2017. https://doi.org/10.1128/mmbr.00002-17.
36. dos Santos WM, Gonzaga MIS, da Silva AJ, de Almeida AQ. Improved water and ions dynamics in a clayey soil amended with different types of agro-industrial waste biochar. Soil Tillage Res. 2022;223:105482. https://doi.org/10.1016/j.still.2022.105482.
37. Long X-X, Yu Z-N, Liu S, Gao T, Qiu R-L. A systematic review of biochar aging and the potential eco-environmental risk in heavy metal contaminated soil. J Hazard Mater. 2024;472:134345. https://doi.org/10.1016/j.jhazmat.2024.134345.
38. Fan J, Duan T, Wu X, Liao M, Sun J. Can the aging process necessarily weaken the effect of Biochar on cadmium-contaminated soil remediation: considering Biochar at different pyrolysis temperatures and aging treatment. Environ Geochem Health. 2025;47:66. https://doi.org/10.1007/s10653-025-02376-1.
39. Prasad MNV. Biochar applications for sustainable agriculture and environmental management. Agroecological approaches for sustainable soil management. John Wiley & Sons, Ltd; 2023. pp. 165–99. https://doi.org/10.1002/9781119911999.ch7.
40. Ding Y, Liu Y, Liu S, Li Z, Tan X, Huang X, et al. Biochar to improve soil fertility. A review. Agron Sustain Dev. 2016;36:36. https://doi.org/10.1007/s13593-016-0372-z.
41. Dai Y, Zheng H, Jiang Z, Xing B. Combined effects of biochar properties and soil conditions on plant growth: a meta-analysis. Sci Total Environ. 2020;713:136635. https://doi.org/10.1016/j.scitotenv.2020.136635.
42. Hossain MZ, Bahar MM, Sarkar B, Donne SW, Ok YS, Palansooriya KN, et al. Biochar and its importance on nutrient dynamics in soil and plant. Biochar. 2020;2:379–420. https://doi.org/10.1007/s42773-020-00065-z.
43. Yuan J, Chen H, Chen G, Pokharel P, Chang SX, Wang Y, et al. Long-term biochar application influences phosphorus and associated iron and sulfur transformations in the rhizosphere. Carbon Res. 2024;3:25. https://doi.org/10.1007/s44246-024-00109-0.
44. Hu Y, Jiang Y, Chhin S, Liu N, Pan H, Zhang J, et al. Alleviating monoculture-induced soil degradation in Chinese Fir plantations in Southern China: optimizing understory mixtures balances stoichiometry and microbial diversity. Ind Crop Prod. 2025;232:121254. https://doi.org/10.1016/j.indcrop.2025.121254.
45. Zhou Y, Yang Z, Liu J, Li X, Wang X, Dai C, et al. Crop rotation and native microbiome inoculation restore soil capacity to suppress a root disease. Nat Commun. 2023;14:8126. https://doi.org/10.1038/s41467-023-43926-4.
46. Parasar BJ, Agarwala N. Unravelling the role of biochar-microbe-soil tripartite interaction in regulating soil carbon and nitrogen budget: a panacea to soil sustainability. Biochar. 2025;7:37. https://doi.org/10.1007/s42773-024-00411-5.
47. Kracmarova-Farren M, Alexova E, Kodatova A, Mercl F, Szakova J, Tlustos P, et al. Biochar-induced changes in soil microbial communities: a comparison of two feedstocks and pyrolysis temperatures. Environ Microbiome. 2024;19:87. https://doi.org/10.1186/s40793-024-00631-z.
48. Campos P, Miller AZ, Prats SA, Knicker H, Hagemann N, De la Rosa JM. Biochar amendment increases bacterial diversity and vegetation cover in trace element-polluted soils: A long-term field experiment. Soil Biol Biochem. 2020;150:108014. https://doi.org/10.1016/j.soilbio.2020.108014.
49. Hu Y, Li Y, Liu K, Shi C, Wang W, Yang Z, et al. Improving the stability of black soil microbial communities through long-term application of biochar to optimize the characteristics of DOM components. Biochar. 2025;7:84. https://doi.org/10.1007/s42773-025-00473-z.
50. Yang L, Ning D, Yang Y, He N, Li X, Cornell CR, et al. Precipitation balances deterministic and stochastic processes of bacterial community assembly in grassland soils. Soil Biol Biochem. 2022;168:108635. https://doi.org/10.1016/j.soilbio.2022.108635.
51. Dini-Andreote F, Stegen JC, van Elsas JD, Salles JF. Disentangling mechanisms that mediate the balance between stochastic and deterministic processes in microbial succession. Proc Natl Acad Sci U S A. 2015;112:E1326-32. https://doi.org/10.1073/pnas.1414261112.
52. Cc GZJB, Q T. Salinity controls soil microbial community structure and function in coastal estuarine wetlands. Environ Microbiol. 2021. https://doi.org/10.1111/1462-2920.15281. 23.
53. Chen Z, Liu J, Sun H, Xing J, Zhang Z, Jiang J. Effects of biochar applied in either rice or wheat seasons on the production and quality of wheat and nutrient status in paddy profiles. Plants. 2023;12:4131. https://doi.org/10.3390/plants12244131.
54. Liu Q, Zhang Y, Liu B, Amonette JE, Lin Z, Liu G, et al. How does biochar influence soil N cycle? A meta-analysis. Plant Soil. 2018;426:211–25. https://doi.org/10.1007/s11104-018-3619-4.
55. Joseph S, Cowie AL, Van Zwieten L, Bolan N, Budai A, Buss W, et al. How biochar works, and when it doesn't: a review of mechanisms controlling soil and plant responses to biochar. GCB Bioenergy. 2021;13:1731–64. https://doi.org/10.1111/gcbb.12885.
56. Stegen JC, Lin X, Konopka AE, Fredrickson JK. Stochastic and deterministic assembly processes in subsurface microbial communities. ISME J. 2012;6:1653–64. https://doi.org/10.1038/ismej.2012.22.

Publisher's Note